Diamond & Related Materials 137 (2023) 110072

Contents lists available at ScienceDirect

Diamond & Related Materials

journal homepage: www.elsevier.com/locate/diamond

4H-SiC Schottky barrier diodes as radiation detectors: A role of Schottky contact area

Ivana Capan [a], Robert Bernat [a], Takahiro Makino [b], Tihomir Knežević [a,*]

[a] Ruđer Bošković Institute, Bijenička 54, 10 000 Zagreb, Croatia
[b] National Institutes for Quantum Science and Technology, 1233 Watanuki, Takasaki, Japan

ARTICLE INFO

Keywords:
Silicon-carbide
4H-SiC
Schottky barrier height
Radiation detection
Deep-level transient spectroscopy (DLTS)

ABSTRACT

Large-area SiC Schottky barrier diodes can significantly improve the sensitivity in radiation detection due to the increased interacting SiC volume. In this work, we tested a large SiC detector with an area of 1 × 1 cm^2. Extensive electrical characterization was performed at temperatures ranging from 150 K to 390 K, demonstrating the impact of barrier inhomogeneities on the electrical performance of the diode. Forward current-voltage (*I-V*) measurements of the diodes revealed two distinct regions caused by Schottky barrier inhomogeneity present throughout the entire temperature range. The barrier heights in the low- and high-current forward voltage regions were extracted from Richardson plots corrected for the Gaussian distribution of barrier heights, yielding values of 1.52 eV and 1.79 eV, respectively. Deep-level transient spectroscopy (DLTS) revealed only one deep-level defect, $Z_{1/2}$, with an activation energy for electron emission of 0.67 eV, which was assigned to the known carbon vacancy. The DLTS study showed no correlation between electrically active defects and barrier inhomogeneity. An excellent energy resolution of 3.2 % was measured using a large area ^{241}Am radiation source, consistent with values for small area SiC detectors that exhibited no barrier height inhomogeneities. The impact of temperature on the alpha particle radiation response was determined within a temperature range of 200 K to 390 K.

1. Introduction

Silicon carbide (SiC) is a wide bandgap semiconductor with several polytypes, the best known of which are 3C, 4H, and 6H. Due to its various interesting properties, such as large critical electric field, high thermal conductivity, high electron saturation velocity, chemical inertness, and radiation hardness, SiC has attracted great interest as a promising material for numerous applications in quantum technology, power electronics, and radiation detection [1–9]. In particular, of all the polytypes, 4H-SiC is ideally suited for radiation detection applications in harsh environments due to its radiation-hardness [10,11].

Among the 4H-SiC-based devices utilized for radiation detection applications, the most widely used are *pin* diodes [12], metal-oxide-semiconductor (MOS) devices [13], and Schottky barrier diodes (SBDs) [9,11,14–19]. While being nearly the simplest electronic device, SBDs have been the most researched and used in recent years. A schematic of a typical n-type 4H-SiC SBD used for radiation detection is shown in Fig. 1.

In addition to the metallization used for the Schottky barrier diode, i.e. Ni, Ti, Mo, geometrical parameters like the contact area and the thickness of the epitaxial layer are crucial for the sensitivity of SBD radiation detectors. The commonly reported values for the thickness of SiC epitaxial layers are a few tenths of micrometers. Recently, 4H-SiC epitaxial layers with thicknesses up to 250 μm used for radiation detection applications have been reported [16,20].

The trend toward increasing the interacting SiC volume is supported by the development of larger area substrates, which now reach 8 in. [21]. Typical values for Schottky contact areas range from 1 to 20 mm^2 [9,11,14–19]. Most studies, reporting on radiation applications, use SiC SBDs with an area of about 15mm^2. Recently, studies on large area Schottky contacts have been reported. Liu et al. [22] have made significant progress with the largest reported area of 1 cm^2 or 4 cm^2 with parallel connection of four 1 cm^2 diodes [23]. Although it would be desirable for radiation applications to increase the Schottky contact area as much as possible, we are still limited in this regard because the contact area strongly affects the electrical properties of the SBDs.

Increasing the Schottky contact area can lead to a higher probability that the metal-semiconductor interface will be affected by surface

* Corresponding author.
E-mail address: tihomir.knezevic@irb.hr (T. Knežević).

https://doi.org/10.1016/j.diamond.2023.110072
Received 7 March 2023; Received in revised form 28 April 2023; Accepted 28 May 2023
Available online 30 May 2023

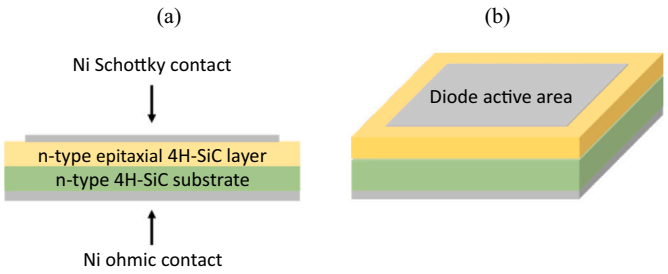

Fig. 1. Schematic of the Schottky barrier diode (a) cross-section and (b) three-dimensional view.

defects [24–26] or other parasitic effects such as doping inhomogeneity [26]. This leads to the formation of barrier height inhomogeneities in SiC SBDs that have been observed to impact the electrical performance and lead to temperature variations of the ideality factor and Schottky barrier height derived from the pure thermionic emission model [27]. The local effects and inhomogeneity at the metal-semiconductor interface decrease the Schottky barrier height and increase the ideality factor, causing the reverse saturation currents of the diode to increase [24–26,28]. Apart from the increase in dark current, the defects leading to barrier inhomogeneity may be electrically active and further degrade the performance of the detector [25,29,30]. However, in some cases, no correlation between electrically active defects and barrier inhomogeneities has been observed [24,31].

In this work, we fabricated a 4H-SiC SBD with one of the largest Schottky contact areas of 1 cm^2. The quality of the SBD was comprehensively investigated using temperature dependent current-voltage (*I-V-T*) and capacitance-voltage (*C-V-T*) measurements, as well as deep-level transient spectroscopy (DLTS) measurements. In addition, the radiation response to alpha particles was investigated in a wide temperature range.

2. Experimental details

We fabricated and characterized an SBD with a large area of 1 × 1 cm^2 on a 25 μm thick n-type nitrogen-doped 4H-SiC epitaxial layer. The SiC epitaxial layers were grown by chemical vapor deposition on an 8° off-cut silicon face of a 350 μm thick 4H-SiC (0001) wafer without a buffer layer. Ohmic contacts were formed on the backside of the SiC substrate by nickel sintering at 950 °C in an Ar atmosphere. The surface was protected during the high temperature treatment for ohmic contact formation. The SBDs were formed by thermal evaporation of nickel with a thickness of 100 nm through a metal mask. The Schottky electrode was not annealed.

The quality of the fabricated large area SBDs was comprehensively evaluated by temperature-dependent current–voltage (*I–V-T*) and capacitance–voltage (*C–V-T*) measurements using a Keithley 4200 SCS (Keithley Instruments, Cleveland, OH, USA). Electrically active defects were characterized by deep-level transient spectroscopy (DLTS). DLTS measurements were performed in the temperature range of 100 to 390 K. The temperature ramp rate was 2 K/min. Capacitance transients were measured using a Boonton (Boonton Electronics, Parsippany, NJ, USA) 7200 capacitance meter with a 30 mV, 1 MHz sinusoidal signal.

The radiation response of 4H-SiC SBDs to alpha particles was measured using a ^{241}Am large area source (active area radius = 25 mm, A = 3.4 kBq). The measurement system for radiation detection consisted of a charge-sensitive preamplifier (CREMAT CR-110), a Gaussian shaping amplifier (CREMAT CR-200-1 s), a multichannel analyzer (AMPTEK MCA 8000D), and a laptop. To minimize the electronic noise, the system was operated with a battery power supply. A DC/DC converter (XP Power CA05P-5), also battery powered, was used to reversely bias the detector to 100 V. The shaping time was 1 s. Radiation response was measured at temperatures from 200 K to 390 K in a cryostat system.

3. Results and discussion

3.1. Impact of area size on electrical characteristics of SBDs

The presence of barrier height inhomogeneity in the large area SBD was confirmed by comparing the forward *I-V* curves with diodes of 1 × 1 mm^2 and 3 × 3 mm^2 area, as shown in Fig. 2. The *I-V* curve of the large area SBD exhibits two distinct regions in the low-current and high-current region attributed to the presence of two different Schottky barrier heights forming a parallel diode connection. The saturation current density of SBD using a pure thermionic emission model is given as follows [27]:

$$I_S = AA^*T^2 exp\left(-\frac{q\phi_B}{kT}\right), \quad (1)$$

where A is the diode area, A^* is the Richardson constant with a value of 146 A cm^{-2} K^{-2} for SiC, T is the temperature, q is the elementary charge, k is the Boltzmann constant, and ϕ_B is the zero bias barrier height. The zero bias barrier height can be calculated as follows:

$$\phi_B = \frac{kT}{q} ln \frac{AA^*T^2}{I_S}. \quad (2)$$

A comparison of the barrier height derived from (2) and the ideality factor of the diodes from Fig. 2 is given in Table 1.

The series resistance of a large-area SBD is 3 Ω determined from the high-current region. The series resistance of the devices with the area of 1 × 1 mm^2 and 3 × 3 mm^2 is extracted to values of 1.2 kΩ and 25 Ω, respectively. The series resistance is seen to impact the electrical characteristics in the high-current region dominantly for the small-area devices. The nitrogen doping of the epitaxial layers of ~1.5 × 10^{14} cm^{-3} was determined from the C—V measurement at room temperature.

3.2. Analysis of Schottky barrier height inhomogeneities

To analyze the impact of Schottky barrier height inhomogeneities in the large-area SBD, the diode was electrically characterized at temperatures from 150 K to 390 K. The forward *I-V-T* measurement of the diodes revealed that two distinct regions exist over the entire temperature range, as shown in Fig. 3. The saturation current density of the Schottky barrier dominates the low-current region and determines the reverse-bias leakage current down to ~40 V, as shown in Fig. 3b for the reverse bias measurements at temperatures from 200 K to 390 K. The temperature dependence of the leakage current after ~60 V reverse bias indicates the impact of tunneling mechanisms on the diode current [25,27]. Other mechanisms, such as generation-recombination

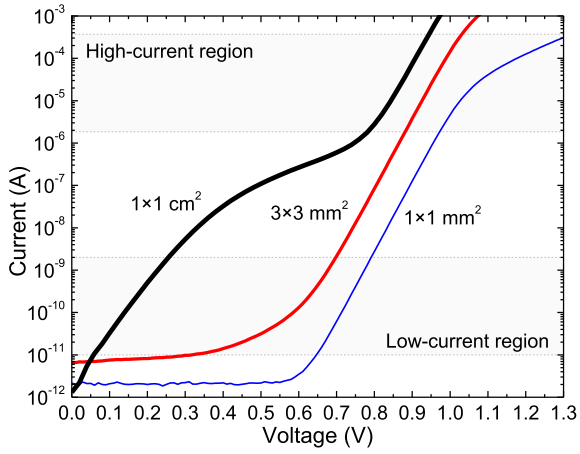

Fig. 2. Forward current-voltage characteristics of SBD with area of 1 × 1 mm^2, 3 × 3 mm^2 and 1 × 1 cm^2 measured at room temperature.

Table 1
Barrier height, ϕ_B, and ideality factor, n, of SBD with different diode area at room temperature.

Diode area	Current region	ϕ_B (eV)	Ideality factor (n)
1×1 mm^2	–	1.59	1.01
3×3 mm^2	–	1.55	1.03
1×1 cm^2	Low-current	1.11	1.46
1×1 cm^2	High-current	1.51	1.06

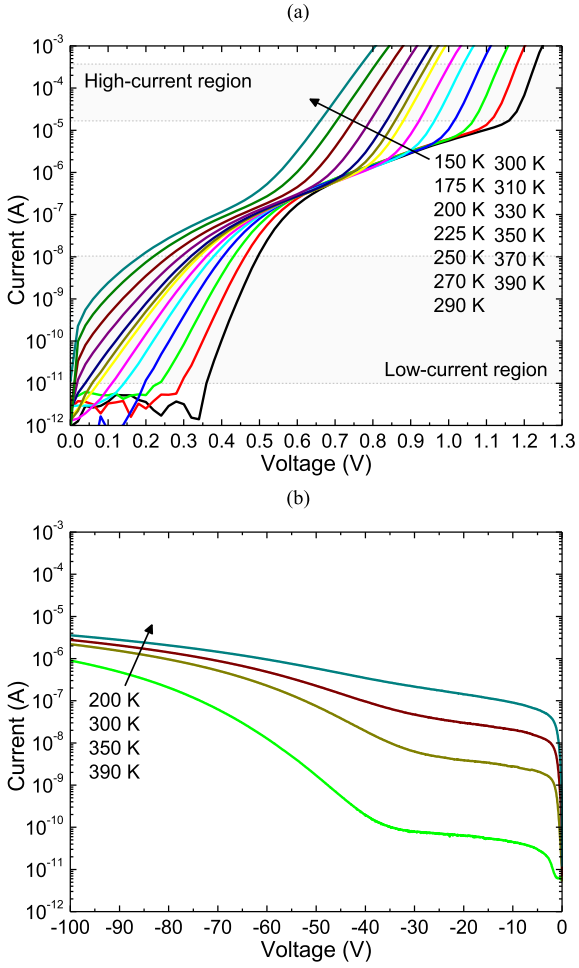

Fig. 3. Current-voltage characteristics of a large 1×1 cm^2 SBD measured at (a) forward bias at temperatures from 150 K to 390 K (b) reverse bias down to 100 V at temperatures from 200 K to 390 K.

processes assisted by defects or trap-assisted tunneling, can also play a role on the observed temperature behavior of the leakage current [27].

The height of the Schottky barrier was determined using (2) for both saturation current densities in the low-current and high-current region for temperatures from 150 K to 330 K and for temperatures from 150 K to 390 K, respectively. For both regions, the height of the Schottky barrier increases with increasing temperature, as shown in Fig. 4. The ideality factor is plotted in the same graph as a function of the measured temperature. The ideality factor of the SBD in the high-current region is lower than the ideality factor of the SBD in the low-current region. This indicates the existence of charge transport mechanisms other than thermionic emission in the low-current region, which can include tunneling or generation-recombination mechanisms [25]. A higher ideality factor, as seen in the low-current region, could also be caused by inhomogeneous variations of the lateral ϕ_B [25,32,33]. These mechanisms can affect the extraction of the ideality factor and the barrier

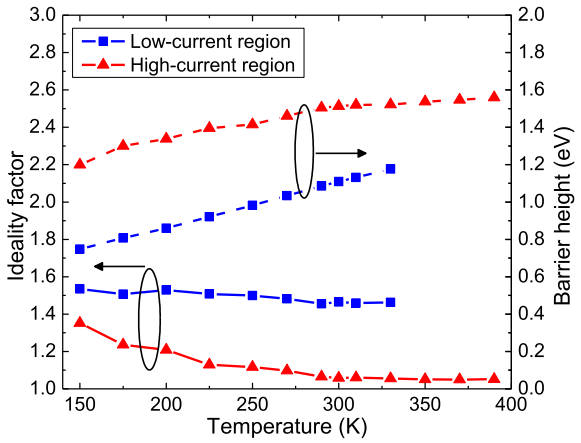

Fig. 4. Ideality factor and barrier height at low- and high-current regions as a function of measurement temperature.

height from the linear part of the semi-logarithmic *I-V* curve in the low-current region, and the values for temperatures above 330 K were not included in the analysis.

Eq. (1) can be written as:

$$ln\left(\frac{I_S}{T^2}\right) = ln(AA^*) - \frac{q\phi_B}{kT}, \tag{3}$$

and the plot of $\ln(I_S/T^2)$ as a function of $1/T$, called the Richardson plot, can be used to extract ϕ_B. The Richardson plot was used to extract the barrier heights in the low- and high-current regions, yielding values of 0.39 eV and 0.99 eV, respectively. The Richardson plot method is not able to determine the exact value of the barrier height due to the barrier height inhomogeneities, resulting in a large discrepancy between the extracted values and the values reported in the literature [34,35].

A model of barrier height that assumes Gaussian spatial distribution of barrier heights across the interface can better explain the temperature dependence of ϕ_B and allows the extraction of the apparent barrier height, $\phi_{B,ap}$ [36]. The standard deviation, σ, and the mean value of the Gaussian distribution of the barrier height, $\overline{\phi_B}$, are determined from the plot of the barrier height as a function of temperature. The values of σ for the low-current and high-current regions are 0.143 V and 0.124 V, respectively. Assuming a Gaussian distribution of barrier heights, Eq. (1) can be rewritten as follows [36]:

$$I_S = AA^*T^2 exp\left[-\frac{q\phi_{B,ap}}{kT} + \frac{q^2\sigma^2}{2k^2T^2}\right]. \tag{4}$$

where the modification for the Richardson plot is given as follows:

$$ln\left(\frac{I_S}{T^2}\right) - \frac{q^2\sigma^2}{2k^2T^2} = ln(AA^*) - \frac{q\phi_{B,ap}}{kT}. \tag{5}$$

The modified Richardson plots are shown in Fig. 5 for both the low- and high-current regions. The apparent barrier heights of 1.52 eV and 1.79 eV were calculated for the low- and high-current regions, respectively, and agree well with the values reported in the literature. The modified Richardson constant was 155 A cm^{-2} K^{-2} for the barrier in the high-current region, assuming an area of 1 cm^2, which agrees with the theoretical value.

3.3. Deep-level transient spectroscopy of large-area SBD

The as-grown large-area 4H-SiC SBD was characterized by deep-level transient spectroscopy (DLTS). The DLTS spectra for emission rates of 10 and 20 s^{-1} are shown in Fig. 6. It is evident that only one DLTS peak with a maximum at around 300 K, known as $Z_{1/2}$, is present in the spectra. The activation energy, E_a, for electron emission and the apparent

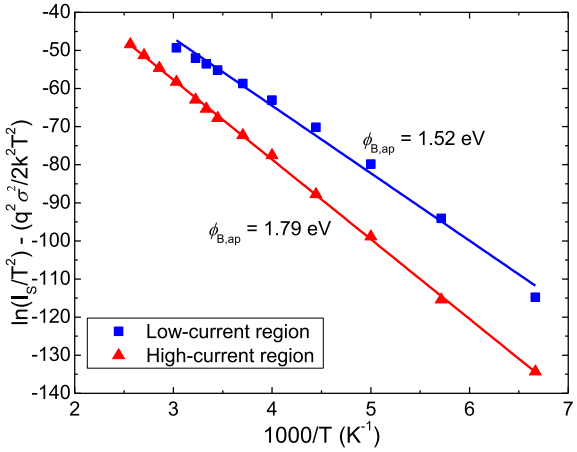

Fig. 5. Modified Richardson plot with the Gaussian distribution of barrier heights across the metal-semiconductor interface.

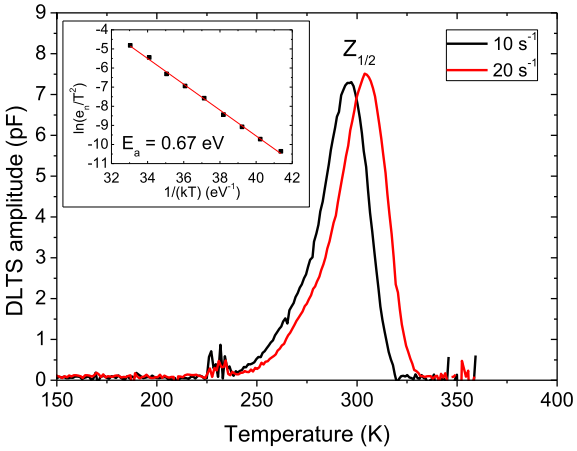

Fig. 6. DLTS spectra for the as-grown 4H-SiC SBD. Measurement settings are V_R = -10 V, V_P = −0.1 V, t_P = 0 ms. Emissions rates are 10 s^{-1} and 20 s^{-1}. Inset: Arrhenius plot of the T^2-corrected electron emission rate.

capture cross sections for the $Z_{1/2}$ deep level were determined from the Arrhenius plot of the T^2-corrected electron emission rate, as shown in the inset of Fig. 6. The activation energy and apparent capture cross section of the $Z_{1/2}$ deep level are E_C - 0.67 eV and 1.04 × 10^{-14} cm^2, respectively.

$Z_{1/2}$ is a well-known deep level defect, and it has already been assigned to the carbon vacancy (V_c) [37–39]. V_c is often referred to as a "lifetime killer" due to its detrimental effect on carrier lifetime [40]. It is one of the most important and dominant defects in 4H-SiC material. It introduces the deep level defect ($Z_{1/2}$), which acts as a very efficient trap or recombination center for the charge carriers. A trap concentration of 7.02 × 10^{12} cm^{-3} was calculated from DLTS measurements.

No correlation was found between the electrically active defects and barrier inhomogeneity in the DLTS study.

3.4. Radiation response of large-area SBD

Irradiations of 4H-SiC SBDs with alpha particles of different energy were performed at a range of temperatures between 200 K and 390 K under a vacuum of less than 0.1 mbar. The distance between the source and the detector was kept at 5 mm. The radiation response to the alpha source ^{241}Am (E_{max} = 5486 keV) is shown in Fig. 7. The energy resolution for ^{241}Am was 3.2 % at 300 K and is consistent with the values of 3 % reported in previous studies where the measurements were performed on small area SiC SBDs in vacuum [41].

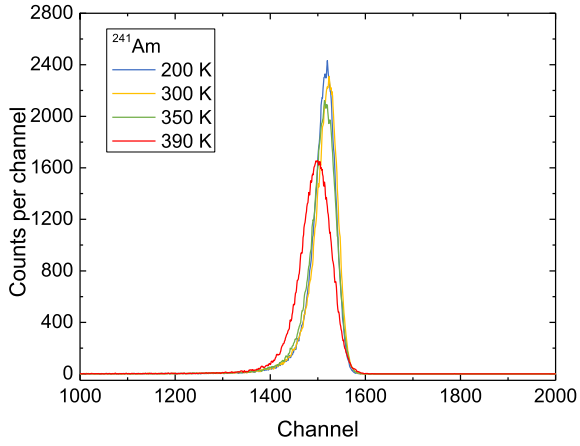

Fig. 7. Radiation response of 4H-SiC detectors with surface area of 1 × 1 cm^2 to ^{241}Am alpha particles at 200 K, 300 K, 350 K and 390 K.

Since the saturation current density of the Schottky barrier dominates the low-current region and determines the reverse-bias leakage current, as shown in Fig. 3b for temperatures from 200 K to 390 K, the impact of temperature on the radiation response of the detector was measured. The radiation response for ^{241}Am was determined at temperatures from 200 K to 390 K, as shown in Fig. 7. The energy resolutions for the radiation response of ^{241}Am at temperatures of 200 K, 300 K, 350 K, and 390 K are 3.2 %, 3.2 %, 3.5 %, and 4.9 %, respectively. Although the leakage current is high at an operating reverse bias voltage of 100 V and increases with temperature, the energy resolution was not significantly affected by operation at elevated temperatures.

4. Conclusions

Extensive electrical characterization of a 1 × 1 cm^2 SBD showed the variation of the ideality factor and Schottky barrier height with temperature. Two different Schottky barriers were identified to affect the forward-bias current in either the low-current or high-current regions. This was explained by an inhomogeneity of the Schottky barrier height at the metal-semiconductor interface. The barrier height inhomogeneity was not readily observed for devices with smaller areas. This is due to the statistical nature of the formation of surface defects or possible doping inhomogeneity, which is thought to lead to the formation of barrier inhomogeneity. Modified Richardson plots were used to determine the apparent barrier heights, assuming a Gaussian variation in barrier inhomogeneity. The apparent barrier heights of 1.52 eV and 1.79 eV were extracted for the low- and high-current regions, respectively. The DLTS study revealed no correlation between barrier height inhomogeneity and electrically active defects. Only one deep-level defect, $Z_{1/2}$, was assigned to the known carbon vacancy with an activation energy for electron emission of 0.67 eV. The radiation response of large area detectors to alpha particles confirmed that the larger Schottky area increases the sensitivity of the detector and that the inhomogeneity of the barrier height does not significantly affect the energy resolution even when the diode is operated at elevated temperatures.

CRediT authorship contribution statement

Ivana Capan: Conceptualization, Data curation, Formal analysis, Funding acquisition, Investigation, Methodology, Project administration, Resources, Supervision, Validation, Visualization, Writing – original draft, Writing – review & editing. **Robert Bernat:** Data curation, Formal analysis, Investigation, Visualization, Writing – original draft, Writing – review & editing. **Takahiro Makino:** Data curation, Formal analysis, Investigation, Resources, Validation, Writing – review &

editing. **Tihomir Knežević:** Data curation, Formal analysis, Investigation, Visualization, Writing – original draft, Writing – review & editing.

Declaration of competing interest

The authors declare that they have no known competing financial interests or personal relationships that could have appeared to influence the work reported in this paper.

Data availability

Data will be made available on request.

Acknowledgments

The present work was financially supported by the NATO Science for Peace and Security Programme, project no. G5674.

References

[1] R. Hedayati, L. Lanni, S. Rodriguez, B. Gunnar Malm, A. Rusu, C.-M. Zetterling, A monolithic, 500 °C operational amplifier in 4H-SiC bipolar technology, IEEE Electron Device Lett. 35 (2014) 693–695, https://doi.org/10.1109/LED.2014.2322335.

[2] S. Sei-Hyung Ryu, B. Krishnaswami, B. Hull, M. Heath, J. Das, H. Fatima Richmond, A. Jon Zhang, J. Agarwal, A. Palmour, B. Lelis, D. Geil, C. Katsis, J. Scofield Scozzie, High speed switching devices in 4H-SiC - performance and reliability, in: 2005 International Semiconductor Device Research Symposium, IEEE, Bethesda, Maryland, USA, 2005, pp. 162–163, https://doi.org/10.1109/ISDRS.2005.1596032.

[3] J. Wang, Y. Zhou, X. Zhang, F. Liu, Y. Li, K. Li, Z. Liu, G. Wang, W. Gao, Efficient generation of an array of single silicon-vacancy defects in silicon carbide, Phys. Rev. Appl. 7 (2017), 064021, https://doi.org/10.1103/PhysRevApplied.7.064021.

[4] M. Widmann, S.-Y. Lee, T. Rendler, N.T. Son, H. Fedder, S. Paik, L.-P. Yang, N. Zhao, S. Yang, I. Booker, A. Denisenko, M. Jamali, S.A. Momenzadeh, I. Gerhardt, T. Ohshima, A. Gali, E. Janzén, J. Wrachtrup, Coherent control of single spins in silicon carbide at room temperature, Nat. Mater. 14 (2015) 164–168, https://doi.org/10.1038/nmat4145.

[5] F. Fuchs, B. Stender, M. Trupke, D. Simin, J. Pflaum, V. Dyakonov, G.V. Astakhov, Engineering near-infrared single-photon emitters with optically active spins in ultrapure silicon carbide, Nat. Commun. 6 (2015) 7578, https://doi.org/10.1038/ncomms8578.

[6] G. Wolfowicz, C.P. Anderson, A.L. Yeats, S.J. Whiteley, J. Niklas, O.G. Poluektov, F. J. Heremans, D.D. Awschalom, Optical charge state control of spin defects in 4H-SiC, Nat. Commun. 8 (2017) 1876, https://doi.org/10.1038/s41467-017-01993-4.

[7] C. Kasper, D. Klenkert, Z. Shang, D. Simin, A. Gottscholl, A. Sperlich, H. Kraus, C. Schneider, S. Zhou, M. Trupke, W. Kada, T. Ohshima, V. Dyakonov, G. V. Astakhov, Influence of irradiation on defect spin coherence in silicon carbide, Phys. Rev. Appl. 13 (2020), 044054, https://doi.org/10.1103/PhysRevApplied.13.044054.

[8] K. Szász, V. Ivády, I.A. Abrikosov, E. Janzén, M. Bockstedte, A. Gali, Spin and photophysics of carbon-antisite vacancy defect in 4 H silicon carbide: a potential quantum bit, Phys. Rev. B 91 (2015), 121201, https://doi.org/10.1103/PhysRevB.91.121201.

[9] V. Radulović, K. Ambrožič, L. Snoj, I. Capan, T. Brodar, Z. Ereš, Ž. Pastuović, A. Sarbutt, T. Ohshima, Y. Yamazaki, J. Coutinho, E-SiCure collaboration project: silicon carbide material studies and detector prototype testing at the JSI TRIGA reactor, EPJ Web Conf. 225 (2020) 07007, https://doi.org/10.1051/epjconf/202022507007.

[10] J. Coutinho, V.J.B. Torres, I. Capan, T. Brodar, Z. Ereš, R. Bernat, V. Radulović, K. Ambrožič, L. Snoj, Ž. Pastuović, A. Sarbutt, T. Ohshima, Y. Yamazaki, T. Makino, Silicon carbide diodes for neutron detection, Nucl. Inst. Methods Phys. Res. A Accelerators Spectrometers Detectors Assoc. Equip. 986 (2021), 164793, https://doi.org/10.1016/j.nima.2020.164793.

[11] I. Capan, 4H-SiC Schottky barrier diodes as radiation detectors: a review, Electronics. 11 (2022) 532, https://doi.org/10.3390/electronics11040532.

[12] R.L. Gao, X. Du, W.Y. Ma, B. Sun, J.L. Ruan, X. Ouyang, H. Li, L. Chen, L.Y. Liu, X. P. Ouyang, Radiation tolerance analysis of 4H-SiC PIN diode detectors for neutron irradiation, Sensors Actuators A Phys. 333 (2022), 113241, https://doi.org/10.1016/j.sna.2021.113241.

[13] S.K. Chaudhuri, O. Karadavut, J.W. Kleppinger, K.C. Mandal, High-resolution radiation detection using Ni/SiO_2/n-4H-SiC vertical metal-oxide-semiconductor capacitor, J. Appl. Phys. 130 (2021), 074501, https://doi.org/10.1063/5.0059151.

[14] F.H. Ruddy, J.G. Seidel, H. Chen, A.R. Dulloo, S.-H. Ryu, High-resolution alpha-particle spectrometry using silicon carbide semiconductor detectors, in: IEEE Nuclear Science Symposium Conference Record, 2005, IEEE, Wyndham El Conquistador Resort, Puerto Rico, 2005, pp. 1231–1235, https://doi.org/10.1109/NSSMIC.2005.1596541.

[15] B. Zaňko, L. Hrubčín, A. Šagátová, J. Osvald, P. Boháček, E. Kováčová, Y. Halahovets, S.V. Rozov, V.G. Sandukovskij, Study of Schottky barrier detectors based on a high quality 4H-SiC epitaxial layer with different thickness, Appl. Surf. Sci. 536 (2021), 147801, https://doi.org/10.1016/j.apsusc.2020.147801.

[16] J.W. Kleppinger, S.K. Chaudhuri, O. Karadavut, K.C. Mandal, Defect characterization and charge transport measurements in high-resolution Ni/n-4H-SiC Schottky barrier radiation detectors fabricated on 250 μ m epitaxial layers, J. Appl. Phys. 129 (2021), 244501, https://doi.org/10.1063/5.0049218.

[17] R. Bernat, I. Capan, L. Bakrač, T. Brodar, T. Makino, T. Ohshima, Ž. Pastuović, A. Sarbutt, Response of 4H-SiC detectors to ionizing particles, Crystals. 11 (2020) 10, https://doi.org/10.3390/cryst11010010.

[18] R.W. Flammang, J.G. Seidel, F.H. Ruddy, Fast neutron detection with silicon carbide semiconductor radiation detectors, Nucl. Inst. Methods Phys. Res. A Accelerators Spectrometers Detectors Assoc. Equip. 579 (2007) 177–179, https://doi.org/10.1016/j.nima.2007.04.034.

[19] J.E. Lees, D.J. Bassford, G.W. Fraser, A.B. Horsfall, K.V. Vassilevski, N.G. Wright, A. Owens, Semi-transparent SiC Schottky diodes for X-ray spectroscopy, Nucl. Inst. Methods Phys. Res. A Accelerators Spectrometers Detectors Assoc. Equip. 578 (2007) 226–234, https://doi.org/10.1016/j.nima.2007.05.172.

[20] A. Meli, A. Muoio, A. Trotta, L. Meda, M. Parisi, F. La Via, Epitaxial growth and characterization of 4H-SiC for neutron detection applications, Materials. 14 (2021) 976, https://doi.org/10.3390/ma14040976.

[21] M. Musolino, X. Xu, H. Wang, V. Rengarajan, I. Zwieback, G. Ruland, D. Crippa, M. Mauceri, M. Calabretta, A. Messina, Paving the way toward the world's first 200mm SiC pilot line, Mater. Sci. Semicond. Process. 135 (2021), 106088, https://doi.org/10.1016/j.mssp.2021.106088.

[22] L. Liu, A. Liu, S. Bai, L. Lv, P. Jin, X. Ouyang, Radiation resistance of silicon carbide Schottky diode detectors in D-T fusion neutron detection, Sci. Rep. 7 (2017) 13376, https://doi.org/10.1038/s41598-017-13715-3.

[23] L.-Y. Liu, L. Wang, P. Jin, J.-L. Liu, X.-P. Zhang, L. Chen, J.-F. Zhang, X.-P. Ouyang, A. Liu, R.-H. Huang, S. Bai, The fabrication and characterization of Ni/4H-SiC Schottky diode radiation detectors with a sensitive area of up to 4 cm2, Sensors. 17 (2017) 2334, https://doi.org/10.3390/s17102334.

[24] V.E. Gora, F.D. Auret, H.T. Danga, S.M. Tunhuma, C. Nyamhere, E. Igumbor, A. Chawanda, Barrier height inhomogeneities on Pd/n-4H-SiC Schottky diodes in a wide temperature range, Mater. Sci. Eng. B 247 (2019), 114370, https://doi.org/10.1016/j.mseb.2019.06.001.

[25] S.K. Mourya, G. Malik, B. Alisha, R. Chandra Kumar, The role of non-homogeneous barrier on the electrical performance of 15R–SiC Schottky diodes grown by in-situ RF sputtering, Mater. Sci. Semicond. Process. 149 (2022), 106855, https://doi.org/10.1016/j.mssp.2022.106855.

[26] H.-J. Im, Y. Ding, J.P. Pelz, W.J. Choyke, Nanometer-scale test of the Tung model of Schottky-barrier height inhomogeneity, Phys. Rev. B 64 (2001), 075310, https://doi.org/10.1103/PhysRevB.64.075310.

[27] S.M. Sze, K.K. Ng, Physics of Semiconductor Devices, 3rd edition, Wiley-Interscience, Hoboken, N.J, 2006.

[28] J. Osvald, L. Hrubčín, B. Zaňko, Temperature dependence of electrical behaviour of inhomogeneous Ni/Au/4H–SiC Schottky diodes, Mater. Sci. Semicond. Process. 140 (2022), 106413, https://doi.org/10.1016/j.mssp.2021.106413.

[29] Ł. Gelczuk, P. Kamyczek, E. Płaczek-Popko, M. Dąbrowska-Szata, Correlation between barrier inhomogeneities of 4H-SiC 1A/600V Schottky rectifiers and deep-level defects revealed by DLTS and Laplace DLTS, Solid State Electron. 99 (2014) 1–6, https://doi.org/10.1016/j.sse.2014.04.043.

[30] M.L. Bolen, M.A. Capano, Defect analysis of barrier height inhomogeneity in titanium 4H-SiC Schottky barrier diodes, J. Elec. Materi. 38 (2009) 574–580, https://doi.org/10.1007/s11664-008-0647-5.

[31] T. Zhang, C. Raynaud, D. Planson, Measure and analysis of 4H-SiC Schottky barrier height with Mo contacts, Eur. Phys. J. Appl. Phys. 85 (2019) 10102, https://doi.org/10.1051/epjap/2018180282.

[32] V.E. Gora, A. Chawanda, C. Nyamhere, F.D. Auret, F. Mazunga, T. Jaure, B. Chibaya, E. Omotoso, H.T. Danga, S.M. Tunhuma, Comparison of nickel, cobalt, palladium, and tungsten Schottky contacts on n-4 H -silicon carbide, Phys. B Condens. Matter 535 (2018) 333–337, https://doi.org/10.1016/j.physb.2017.08.024.

[33] R.F. Schmitsdorf, Explanation of the linear correlation between barrier heights and ideality factors of real metal-semiconductor contacts by laterally nonuniform Schottky barriers, J. Vac. Sci. Technol. B. 15 (1997) 1221, https://doi.org/10.1116/1.589442.

[34] X. Deng, L. Yang, Y. Wen, X. Li, F. Yang, H. Wu, H. Cao, J. Li, W. Chen, B. Zhang, Experimental study and characterization of an ultrahigh-voltage Ni/4H–SiC junction barrier Schottky rectifier with near ideal performances, Superlattice. Microst. 138 (2020), 106381, https://doi.org/10.1016/j.spmi.2019.106381.

[35] S.A. Reshanov, G. Pensl, K. Danno, T. Kimoto, S. Hishiki, T. Ohshima, H. Itoh, F. Yan, R.P. Devaty, W.J. Choyke, Effect of the Schottky barrier height on the detection of midgap levels in 4H-SiC by deep level transient spectroscopy, J. Appl. Phys. 102 (2007), 113702, https://doi.org/10.1063/1.2818050.

[36] J.H. Werner, H.H. Güttler, Barrier inhomogeneities at Schottky contacts, J. Appl. Phys. 69 (1991) 1522–1533, https://doi.org/10.1063/1.347243.

[37] N.T. Son, X.T. Trinh, L.S. Løvlie, B.G. Svensson, K. Kawahara, J. Suda, T. Kimoto, T. Umeda, J. Isoya, T. Makino, T. Ohshima, E. Janzén, Negative- U system of carbon vacancy in 4 H -SiC, Phys. Rev. Lett. 109 (2012), 187603, https://doi.org/10.1103/PhysRevLett.109.187603.

[38] I. Capan, T. Brodar, J. Coutinho, T. Ohshima, V.P. Markevich, A.R. Peaker, Acceptor levels of the carbon vacancy in 4 *H* -SiC: combining Laplace deep level transient spectroscopy with density functional modeling, J. Appl. Phys. 124 (2018), 245701, https://doi.org/10.1063/1.5063773.

[39] I. Capan, T. Brodar, Ž. Pastuović, R. Siegele, T. Ohshima, S. Sato, T. Makino, L. Snoj, V. Radulović, J. Coutinho, V.J.B. Torres, K. Demmouche, Double

negatively charged carbon vacancy at the h- and k-sites in 4H-SiC: combined Laplace-DLTS and DFT study, J. Appl. Phys. 123 (2018), 161597, https://doi.org/10.1063/1.5011124.

[40] T. Kimoto, K. Danno, J. Suda, Lifetime-killing defects in 4H-SiC epilayers and lifetime control by low-energy electron irradiation: lifetime-killing defects in 4H-SiC epilayers and lifetime control, Phys. Stat. Sol. (b). 245 (2008) 1327–1336, https://doi.org/10.1002/pssb.200844076.

[41] R. Bernat, L. Bakrač, V. Radulović, L. Snoj, T. Makino, T. Ohshima, Ž. Pastuović, I. Capan, 4H-SiC Schottky barrier diodes for efficient thermal neutron detection, Materials. 14 (2021) 5105, https://doi.org/10.3390/ma14175105.